

# Neutron capture by Ru: Neutron cross sections of $^{96,102,104}\text{Ru}$ and $\gamma$ -ray spectroscopy in the decays of $^{97,103,105}\text{Ru}$

K. S. Krane

*Department of Physics, Oregon State University, Corvallis, Oregon 97331, USA*

(Received 5 February 2010; published 21 April 2010)

Cross sections for radiative capture of neutrons have been measured for stable isotopes of Ru with mass numbers 96, 102, and 104. From separate irradiations using thermal and epithermal neutrons, independent values for the thermal cross section and effective resonance integral have been determined. Spectroscopic studies of the  $\gamma$  rays emitted in the decays of  $^{97,103,105}\text{Ru}$  have enabled improvements in the precision of the energies and intensities of the radiations along with corresponding improvements in the  $\beta$ -decay feeding intensities and the energies of the levels in the respective daughter nuclei. Similar spectroscopic measurements of the decays of  $^{105}\text{Rh}$  (daughter of  $^{105}\text{Ru}$ ) and  $^{96}\text{Tc}$  (produced from  $n, p$  reactions on  $^{96}\text{Ru}$ ) have resulted in improved  $\gamma$ -ray energies and intensities in those decays.

DOI: [10.1103/PhysRevC.81.044310](https://doi.org/10.1103/PhysRevC.81.044310)

PACS number(s): 25.40.Lw, 27.60.+j, 23.20.Lv

## I. INTRODUCTION

The cross section for the radiative capture of thermal neutrons can be of fundamental importance to the study of nuclear structure and also of practical significance, for example, in geophysics. Neutron capture by the element ruthenium is of particular interest because it has been suggested by Bereznai *et al.* [1] that Ru can serve as a comparator in the quantitative analysis for other elements in neutron activation analysis. Moreover, the need to determine small concentrations of Ru in geological samples has been discussed by Gijbels and Zels [2]; for this determination, precise knowledge of the values of the Ru cross sections is critical.

Unfortunately, there are disagreements, sometimes exceeding 30%, among the previously measured values of the cross sections, as well as between some of the experimental values and the recommended values [3,4]. Moreover, changes in the values of analysis parameters such as half-lives and isotopic abundances have occurred since the reports of previous measurements have been issued. Hence, a new measurement and re-evaluation are called for. The present work describes measurements of the thermal capture cross sections of the stable Ru isotopes with mass numbers 96, 102, and 104 by the activation method. A precise determination of the thermal cross section by activation generally requires correction for captures by epithermal neutrons. As a result, the present work also describes a redetermination of the Ru resonance integrals.

The radioisotopes produced by neutron activation of Ru (namely,  $^{97,103,105}\text{Ru}$ ) have been monitored in the present work by observing their  $\gamma$ -ray spectra, the energies and intensities from which have been previously reported in the literature and summarized in data compilations. The superior efficiency and energy resolution of the Ge spectroscopy system used in the present work has resulted in  $\gamma$ -ray spectroscopic data with improved energies and intensities, and they yield corresponding improvements in the precision of the energy levels in the daughter isotopes and  $\beta$ -decay intensities feeding those levels. The present report includes a summary of these  $\gamma$ -ray energies and intensities, along with the deduced energy levels and  $\beta$ -decay feedings.

## II. EXPERIMENTAL DETAILS

Samples of Ru metal (sponge or powder) or  $\text{RuO}_2$  powder of natural isotopic abundance ranging from 5 to 20 mg were irradiated in the Oregon State University TRIGA reactor [5]. Three different irradiation facilities were used: a thermal column (TC; nominal thermal and epithermal neutron fluxes of respectively  $6.4 \times 10^{10}$  and  $1.8 \times 10^8$  neutrons/cm<sup>2</sup>/s), a cadmium-lined in-core irradiation tube (CLICIT; 0 and  $1.2 \times 10^{12}$  neutrons/cm<sup>2</sup>/s), and a fast pneumatic transfer facility (“rabbit”;  $1.0 \times 10^{13}$  and  $3.5 \times 10^{11}$  neutrons/cm<sup>2</sup>/s). The rabbit samples could also be enclosed in a Cd box (1 mm wall thickness) to isolate the epithermal component.

All Ru irradiations were accompanied with flux monitors. Primary flux monitors were Au and Co as dilute (respectively, 0.134% and 0.438%) alloys in thin Al metal foils. In the analysis, the thermal cross section and resonance integral of Au have been assumed to be, respectively,  $98.65 \pm 0.09$  b and  $1550 \pm 28$  b and those of Co to be, respectively,  $37.18 \pm 0.06$  b and  $74 \pm 2$  b [3]. Zr served as a secondary flux monitor, especially for correcting for the small epithermal components in the TC and rabbit facilities. Irradiations for the cross-section measurements typically lasted 1–3 h in the CLICIT and TC facilities, and counting began within 3 h for some samples and within 15 h for others. Irradiations in the rabbit facility were of 1- to 10-min duration, and counting began within 1 h following the irradiations.

The  $\gamma$  rays were observed with a high-purity Ge detector (nominal volume of 169 cm<sup>3</sup>, efficiency of 35% compared with NaI at 1332 keV, resolution of 1.68 keV at 1332 keV). Source-to-detector distances for the cross-section measurements were generally 10 to 20 cm, for which coincidence-summing effects are negligible. The signals were analyzed with a digital spectroscopy system connected to a desktop computer. Peak areas of the  $\gamma$ -ray lines, which were well isolated from neighboring peaks, were determined with the ORTEC MAESTRO software [6].

Properties of the Ru isotopes used in the cross-section analysis are listed in Table I, taken mostly from the Nuclear Data Sheets (NDS) [7–9] or from the on-line Evaluated Nuclear Structure Data File compilation [10]. (In Table I and

TABLE I. Properties of Ru isotopes.

Capture by	Abundance (%)	Half-life	Analyzing $\gamma$ rays
$^{96}\text{Ru}$	5.54 <i>14</i>	2.838 <i>1</i> d	215.7 (85.6%), 324.5 (10.8%)
$^{102}\text{Ru}$	31.55 <i>14</i>	39.26 <i>2</i> d	497.1 (91.0%), 610.3 + 612.0 (5.87%)
$^{104}\text{Ru}$	18.62 <i>27</i>	4.44 <i>2</i> h	676.4 (15.7%), 724.3 (47.3%)

all following tables in the present work, uncertainties in the least significant digit or digits are indicated in italics.) The  $^{97}\text{Ru}$  half-life is taken from a recent measurement by Goodwin *et al.* [11], which differs from the previous NDS value ( $2.9 \pm 0.1$  d) by about 2.1%. The isotopic abundances are taken from the current IUPAC Commission on Isotopic Abundances and Atomic Weights recommended values [12]. The value of the branching ratio of the 215.7-keV  $\gamma$  ray in the  $^{97}\text{Ru}$  decay, 85.6(9)%, was deduced from the present work.

After correcting for the decay of the sample and the  $\gamma$ -ray branching and efficiency factors, the deduced activities were analyzed according to the result of solving the rate equation for a simple capture and decay process, for which the activity  $a$  is

$$a = N(\sigma\phi_{\text{th}} + I\phi_{\text{epi}})(1 - e^{-\lambda t_i}), \quad (1)$$

where  $N$  (assumed to be constant) is the number of stable Ru target nuclei in the irradiated sample,  $\phi_{\text{th}}$  and  $\phi_{\text{epi}}$  are the thermal and epithermal neutron fluxes, respectively,  $\sigma$  and  $I$  are, respectively, the effective thermal cross section and resonance integral, and  $t_i$  is the irradiation time.

Because there are no broad or low-lying neutron resonances known for any of the Ru isotopes considered in the present work, the cross section closely follows the  $1/v$  behavior below about 1 eV. Therefore, the effective thermal cross section characterizes the entire thermal region. (This is equivalent to setting Wescott's  $g$  factor equal to unity [13].) The effects of neutron absorption within the samples are also negligible, given the thin samples used in the present experiments.

The effective resonance integral  $I$  includes a small contribution from the  $1/v$  region. Assuming the Cd cut-off energy to be about 0.5 eV, this contribution amounts to about  $0.45\sigma$ ; the corrected resonance integral  $I'$  is then

$$I' = I - 0.45\sigma. \quad (2)$$

Because the resonance integral is larger than the thermal cross section, this correction is small—less than 1 standard deviation of the resonance integral for  $^{96}\text{Ru}$  and  $^{104}\text{Ru}$  and slightly above 1 standard deviation for  $^{102}\text{Ru}$ .

Uncertainties in the cross sections depend on a number of factors: isotopic abundance, half-life, flux determinations (including corrections of thermal cross sections for the presence of epithermal neutrons), detector efficiencies, and decay scheme factors, including  $\gamma$ -ray branching. Overall, these factors combine to give a typical uncertainty of 4–5%.

For the  $^{105}\text{Ru}$  spectroscopy studies, samples of typical initial activity of 20  $\mu\text{Ci}$  were counted, beginning at a source-to-detector distance of 25 cm and then moving successively to 20, 15, 10, and 7.5 cm at intervals of approximately one half-life. This procedure enabled sum peaks and long-lived

impurities to be identified readily. Other samples were counted for 12–15 h in a fixed location (usually 15 cm) to enable the half-lives of the lines to be tracked. For the  $^{97}\text{Ru}$  and  $^{103}\text{Ru}$  spectroscopy studies, samples of initial activity 14–28  $\mu\text{Ci}$  were counted at distances of 25, 20, and 15 cm for several days. The samples also contained activities of  $^{96}\text{Tc}$  ( $t_{1/2} = 4.28$  d), probably produced through  $^{96}\text{Ru}(n, p)$ , and  $^{105}\text{Rh}$  ( $t_{1/2} = 35.36$  h), daughter activity of  $^{105}\text{Ru}$ . The present data also give improved values for energies and intensities of the  $\gamma$  rays emitted in these decays. As a result of a small Ir impurity in the Ru, activities of 74-d  $^{192}\text{Ir}$  (initially 0.7  $\mu\text{Ci}$ ) and 19-h  $^{194}\text{Ir}$  (initially 1.0  $\mu\text{Ci}$ ) were also produced in the spectroscopy irradiations. The Ir  $\gamma$  rays occasionally interfered with the measurements of some of the Ru  $\gamma$  rays, but also provided an additional energy calibration.

The  $\gamma$ -ray spectra were analyzed for peak locations and areas using the fitting code SAMPO [14]. Energy calibrations for the spectroscopy studies were done by counting Ru samples simultaneously with samples of  $^{133}\text{Ba}$  and  $^{152}\text{Eu}$  [15]. From these experiments the energies of the strongest lines in the decays could be determined. These energies were in turn used to determine the energies of the weaker lines in longer runs counting only the Ru sources. The minimum energy uncertainty has been set at 10 eV.

Efficiency calibrations were done with sources of  $^{133}\text{Ba}$  and  $^{152}\text{Eu}$ . The calibration below 200 keV was also characterized using reactor-produced sources of  $^{160}\text{Tb}$ ,  $^{169}\text{Yb}$ , and  $^{182}\text{Ta}$ . The minimum uncertainty in intensities for the spectroscopic studies has been set at 2% for energies below 200 keV and 1% above 200 keV. This represents primarily the fitting uncertainty in the efficiency calibrations.

### III. CROSS-SECTION RESULTS

The thermal cross sections of the Ru isotopes were measured through irradiations of several samples each in the TC and rabbit facilities. The average values of the cross sections determined in the present work are shown in Table II in comparison with the results of previous studies [16–23]. The present measured value for the  $^{96}\text{Ru}$  cross section is somewhat smaller than the most precise of the previously measured values. For  $^{102}\text{Ru}$ , the present result agrees somewhat better with the measurement of De Corte and Simonits [20], but for  $^{104}\text{Ru}$  the agreement is slightly better with the previous result of Heft [19]. The disagreements among these results are discussed at greater length in Sec. V.

The resonance integrals were measured through several irradiations in the CLICIT and rabbit facilities (samples for the latter were encased in Cd). The results are shown in

TABLE II. Measured values of Ru thermal cross sections.

Target	Thermal cross section $\sigma$ (b)	
	Present work	Previous work
$^{96}\text{Ru}$	0.207 10	0.210 32, <sup>a</sup> 0.271 27, <sup>b</sup> 0.29 2, <sup>c</sup> 0.218 4, <sup>d</sup> 0.229 3 <sup>e</sup>
$^{102}\text{Ru}$	1.14 5	1.50 23, <sup>a</sup> 1.23 12, <sup>f</sup> 1.37 13, <sup>g</sup> 1.21 7, <sup>c</sup> 1.31 3, <sup>d</sup> 1.16 3 <sup>e</sup>
$^{104}\text{Ru}$	0.468 19	0.47, <sup>h</sup> 0.32 2, <sup>c</sup> 0.466 15, <sup>d</sup> 0.491 10 <sup>e</sup>

<sup>a</sup>Katcoff and Williams [16].<sup>b</sup>Halperin and Druschel [17].<sup>c</sup>Rambaek and Steinnes [18].<sup>d</sup>Heft [19].<sup>e</sup>DeCorte and Simonits [20].<sup>f</sup>Lantz [21].<sup>g</sup>Ishikawa [22].<sup>h</sup>Lantz [23].

Table III and compared with previous values [17–24]. The previous results have been measured by activation, except that of Anufriev *et al.* [24], which was deduced from the measured resonance energies. The variations among the values determined in the cited studies may reflect differences in the epithermal spectra of the various reactors. (The deduced thermal cross sections are unaffected by local differences in the thermal spectrum, as long as there are no low-lying resonances so that the cross section in the thermal region varies as  $1/v$ .)

Based on the current results, we find the resonance integrals corrected for the  $1/v$  contribution to be

$$I'(^{96}\text{Ru}) = 7.12 \pm 0.36 \text{ b},$$

$$I'(^{102}\text{Ru}) = 4.34 \pm 0.24 \text{ b},$$

$$I'(^{104}\text{Ru}) = 6.82 \pm 0.35 \text{ b}.$$

Only in the case of  $^{102}\text{Ru}$  does the correction exceed 1 standard deviation.

#### IV. $\gamma$ -RAY SPECTROSCOPY RESULTS

##### A. $^{97}\text{Ru}$ decay

Figure 1 shows a  $\gamma$ -ray spectrum from the sample about 1 day following the irradiation, by which time the  $^{105}\text{Ru}$  activity had mostly decayed away. The present results for

TABLE III. Measured resonance integrals of Ru.

Target	Resonance integral $I$ (b)	
	Present work	Previous work
$^{96}\text{Ru}$	7.21 36	5.51 39, <sup>a</sup> 7.34 8, <sup>b</sup> 7.0 3, <sup>c</sup> 6.12 23 <sup>d</sup>
$^{102}\text{Ru}$	4.85 24	4.2 1, <sup>b</sup> 4.68 75, <sup>c</sup> 4.21, <sup>d</sup> 4.14 41, <sup>e</sup> 5.5 5 <sup>f</sup>
$^{104}\text{Ru}$	7.03 35	4.3 1, <sup>b</sup> 7.70 65, <sup>c</sup> 6.28 21, <sup>d</sup> 4.6 <sup>g</sup>

<sup>a</sup>Halperin and Druschel [17].<sup>b</sup>Rambaek and Steinnes [18].<sup>c</sup>Heft [19].<sup>d</sup>DeCorte and Simonits [20].<sup>e</sup>Lantz [21].<sup>f</sup>Anufriev *et al.* [24].<sup>g</sup>Lantz [23].

the  $\gamma$ -ray energies and intensities in the decay of 2.8-d  $^{97}\text{Ru}$  are listed in Table IV and compared with previous results taken from the NDS compilation [7], which are consensus values obtained from measurements reported by Cook *et al.* [25], Phelps and Sarantites [26], and Huber and Krämer [27]. Overall, the present results are in good agreement with previous results but have improved the precision on the energies and intensities by factors of typically 2–5. The previously reported weak  $\gamma$  rays at 114.4, 185.0, 483.8, 850.1, and 969.7 keV could not be observed in the present study. The first two (114.4 and 185.0 keV) were previously observed only through  $\gamma\gamma$  coincidences, and the lines at 483.8 and 850.1 keV were obscured respectively by the strong lines at 484.6 keV from the  $^{192}\text{Ir}$  activity and 849.9 keV from the  $^{96}\text{Tc}$  activity. The present data yield an upper limit on the 185-keV intensity that is somewhat smaller than that reported previously by Huber and Krämer, but their result, which is listed in Table IV, is only 2 standard deviations from zero.

Table V lists the energy levels in  $^{97}\text{Tc}$  deduced from the presently measured  $\gamma$ -ray energies. The level energies have been adjusted so that the measured  $\gamma$ -ray energies  $E_\gamma$  agree as closely as possible with the differences  $\Delta E$  between the level energies. The resulting comparison between the  $E_\gamma$  and the  $\Delta E$  shows a normalized  $\chi^2$  of 0.5 and only one case with a difference larger than 1 standard deviation. From the present  $\gamma$ -ray intensities,  $\beta$ -decay feeding intensities and

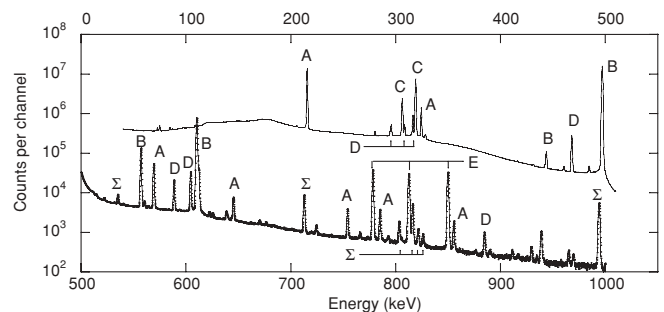


FIG. 1.  $\gamma$ -ray spectrum from irradiated Ru about 1 d after irradiation. Lines identified are A,  $^{97}\text{Ru}$ ; B,  $^{103}\text{Ru}$ ; C,  $^{105}\text{Rh}$ ; D,  $^{192}\text{Ir}$ ; E,  $^{96}\text{Tc}$ . Lines marked with  $\Sigma$  are attributable to coincidence summing.

TABLE IV. Energies and intensities of  $\gamma$  rays emitted in the decay of  $^{97}\text{Ru}$ .

Previous work <sup>a</sup>		Present work		Levels <sup>b</sup>	
$E$ (keV)	$I$	$E$ (keV)	$I$	Initial	Final
108.79 3	0.140 15	108.714 12	0.152 3	D	C
114.4 2	0.0020 4		<0.01	J	H
185.00 1	0.0054 25		<0.001	J	G
215.70 3	100	215.769 10	100.0 10	C	A
324.49 4	12.6 2	324.500 10	12.6 1	D	A
460.56 4	0.141 4	460.546 10	0.155 2	G	D
483.76 10	0.0023 3			E	B
531.06 9	0.0031 3			H	D
560.34 4	0.038 3	560.327 14	0.038 1	F	B
569.29 4	1.02 2	569.272 10	1.05 1	G	C
639.72 2	0.0098 7	639.609 28	0.0091 4	H	C
645.23 5	0.072 4	645.307 10	0.080 1	J	D
670.21 2	0.0100 4	670.192 15	0.0101 3	K	D
753.99 3	0.088 3	754.030 10	0.092 1	J	C
785.05 4	0.084 3	785.016 10	0.094 1	G	A
850.1 4	0.0016 13			I	B
855.44 6	0.050 1	855.423 10	0.0505 5	H	A
898.08 19	0.00021 6		<0.002	K	B
969.65 18	0.00093 10		<0.001	J	A

<sup>a</sup>From NDS compilation [7].<sup>b</sup>See Table V for identification of levels.

the corresponding  $\log ft$  values have been deduced; these are shown in Table V.

### B. $^{103}\text{Ru}$ decay

Table VI shows the present results for the energies and intensities of the  $\gamma$  rays emitted in the decay of 39-d  $^{103}\text{Ru}$ , along with comparison values from the 2001 NDS compilation [8], which is based on energies taken mainly from the work of Macias *et al.* [28] and intensities from the work of Chand *et al.* [29] (The 2009 NDS compilation is based on a preliminary report of this work, which differs from the present report only in the energy uncertainty of the 114.870-keV transition and

TABLE VI. Energies and intensities of  $\gamma$  rays emitted in the decay of  $^{103}\text{Ru}$ .

Previous work <sup>a</sup>		Present work		Levels <sup>b</sup>	
$E$ (keV)	$I$	$E$ (keV)	$I$	Initial	Final
39.760 10	0.0760 11				B A
42.63 4	0.0057 6				H G
53.275 10	0.487 11	53.286 10	0.50 12		C B
62.41 3	0.000 48 4				E D
113.25 7	0.0039 8	113.191 36	0.0035 3		H F
114.97 2	0.0081 5	114.870 25	0.0091 3		I F
241.88 5	0.0198 14	241.875 10	0.0157 3		F D
292.7 2	0.0063 3				0.001 1 H E
294.98 2	0.333 5	294.964 10	0.317 3		D A
317.77 22	0.021 10		<0.01		E B
357.39 14	0.0103 6	357.382 23	0.0095 4		E A
443.80 2	0.379 4	443.810 10	0.373 4		F C
497.084 6	100.0 11	497.085 10	100.0 10		F B
514.60 15	0.0125 16	514.365 12	0.0068 1		G C
557.04 2	0.954 11	557.057 10	0.924 9		H C
567.87 13	0.0031 1	567.693 29	0.0023 1		G B
610.33 2	6.33 5	610.333 10	6.15 6		H B
612.02 2	0.118 3	612.094 60	0.115 6		I B
651.8 4	0.0076 25	651.690 150	0.00024 3		I A

<sup>a</sup>From NDS compilation [8].<sup>b</sup>See Table VII for identification of levels.

in the deduced energy of the 651.731-keV level.) Overall, the present energies are in good agreement with the results of Macias *et al.*; the uncertainties in the present energy values are smaller than those of the previous work by typically factors of 2–5. For the 53-keV transition, a large uncertainty in the presently deduced intensity results from the correction owing to self-absorption in the powder sample.

The present intensity values differ in several instances from those of Chand *et al.* and in fact agree better with the previous (but less precise) intensities reported by Macias *et al.*, notably in the following cases (energies given in keV, intensity values of Macias *et al.* in parentheses with uncertainties in italics): 241.9 (0.0165 17), 292.7 (0.003 3), 514.6 (0.0054 15), 567.9

TABLE V. Energy levels of  $^{97}\text{Tc}$  populated in the decay of  $^{97}\text{Ru}$ .

Level	Previous work <sup>a</sup>			Present work			
	$E$ (keV)	$J^\pi$	$I_{\beta+\epsilon}$	$\log ft$	$E$ (keV)	$I_{\beta+\epsilon}$	$\log ft$
A	0.000	9/2 <sup>+</sup>			0.000		
B	96.560 60	1/2 <sup>-</sup>	0.006 6	>10.1	96.560 60 <sup>a</sup>	0.006 6 <sup>a</sup>	>10.1 <sup>a</sup>
C	215.712 19	7/2 <sup>+</sup>	87.68 5	5.53 2	215.769 10	87.66 11	5.510 9
D	324.479 21	5/2 <sup>+</sup>	11.01 17	6.31 2	324.500 10	11.01 12	6.296 12
E	580.190 60	3/2 <sup>-</sup>	0.0020 3	9.70 7	580.190 60	0.00198 26	9.68 7
F	656.900 60	5/2 <sup>-</sup>	0.033 3	8.34 5	656.887 60	0.0327 10	8.33 2
G	785.048 24	5/2 <sup>+</sup>	1.062 18	6.53 2	785.030 10	1.117 14	6.49 3
H	855.440 30	7/2 <sup>+</sup>	0.0521 12	7.62 3	855.423 10	0.0520 10	7.60 4
I	946.690 110	3/2 <sup>-</sup>	0.0014 11	8.8 4	946.690 110	0.0014 11	8.7 4
J	969.700 40	7/2 <sup>+</sup>	0.099 5	6.76 5	969.803 10	0.151 3	6.56 7
K	994.690 30	(3/2)	0.0087 3	7.61 5	994.692 15	0.00883 31	7.60 9

<sup>a</sup>From NDS compilation [7].

TABLE VII. Energy levels of  $^{103}\text{Rh}$  populated in the decay of  $^{103}\text{Ru}$ .

Level	Previous work <sup>a</sup>				Present work		
	$E$ (keV)	$J^\pi$	$I_\beta$ (%)	$\text{Log } ft$	$E$ (keV)	$I_\beta$ (%)	$\text{Log } ft$
A	0.000	$1/2^-$	0.87 5	9.53 3	0.000	0.87 5 <sup>a</sup>	9.52 3
B	39.756 6	$7/2^+$			39.756 6 <sup>a</sup>		
C	93.041 9	$9/2^+$			93.041 9 <sup>a</sup>		
D	294.980 20	$3/2^-$	0.243 9	9.346 23	294.964 10	0.280 5	9.276 11
E	357.408 20	$5/2^-$	0.007 4	10.68 25	357.382 23	0.0083 5	10.59 3
F	536.838 9	$5/2^+$	92.2 4	5.74 3	536.843 8	92.0 2	5.721 13
G	607.450 40	$(5/2^+, 7/2, 9/2)$	<0.003	>9.4	607.414 13	0.0031 2	9.68 4
H	650.085 16	$7/2^+$	6.61 19	5.95 6	650.093 9	6.50 6	5.93 3
I	651.798 18	$(3/2)^+$	0.091 10	7.79 8	651.731 24	0.110 5	7.68 4

<sup>a</sup>From NDS compilation [8].

(0.0018 8), 651.8 (0.000 19 8). Interference from the strong 316.5-keV transition from  $^{192}\text{Ir}$  prevented any conclusions from the present work regarding the 317.7-keV transition of  $^{103}\text{Ru}$ . Correcting for the 612.5-keV transition of  $^{192}\text{Ir}$  limited the precision of the deduced energy of the 612.0-keV transition of  $^{103}\text{Ru}$ .

The energy levels and  $\beta$  feeding intensities deduced from the present data are shown in Table VII.

### C. $^{105}\text{Ru}$ decay

The  $^{105}\text{Ru}$   $\gamma$ -ray spectrum from an irradiated sample is shown in Fig. 2. Table VIII gives the present results for the energies and intensities of the  $\gamma$  rays emitted in the decay of  $^{105}\text{Ru}$  and a comparison with the previous results from the NDS [9], which are taken mostly from the results of  $\gamma$ -ray singles and coincidence measurements reported by Aras and Walters [30], referred to hereafter as AW. Conversion electron and  $\gamma$ -ray measurements were done by Schriber and Johns [31], referred to as SJ.

Overall, the present data mostly agree with, but are more precise than, the previous work by about an order of magnitude in both the energies and intensities of the emitted  $\gamma$  rays. The following exceptions should be noted:

**129.6 keV.** The presently measured energy of 129.624 keV agrees very well with that of AW ( $129.61 \pm 0.07$  keV) but

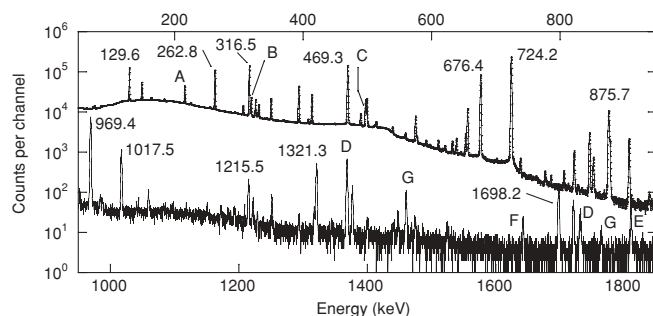


FIG. 2.  $\gamma$ -ray spectrum showing  $^{105}\text{Ru}$  lines soon after irradiation of Ru sample. Energies of some  $^{105}\text{Ru}$  lines are marked. Other lines present are from: A,  $^{97}\text{Ru}$ ; B,  $^{105}\text{Rh}$ ; C,  $^{103}\text{Ru}$ ; D,  $^{24}\text{Na}$ ; E,  $^{56}\text{Mn}$ ; F,  $^{38}\text{Cl}$ ; G, background.

disagrees with the adopted value of  $129.782 \pm 0.004$  keV in the current NDS compilation [9], which was based on the work of Börner *et al.* [32], who used a curved crystal spectrometer to obtain precise  $\gamma$ -ray energies from a source containing a mixture of many fission products. A less precise value ( $129.57 \pm 0.08$  keV) measured by Wilhelmy [33] from the decay of the 45-s  $^{105}\text{Rh}$  isomer also somewhat favors the present value. An independent check of this energy can be obtained from the energy difference of two  $\gamma$  rays from the same excited level that feed the ground state and isomer; the only case in the  $^{105}\text{Ru}$  decay in which this can be done with high precision is for the decays leading from the level at 805.975 keV, for which the decay  $\gamma$  rays give  $\Delta E = 805.973 \pm 0.014 - 676.355 \pm 0.010 = 129.618 \pm 0.017$  keV, in excellent agreement with the value measured directly.

**350 keV doublet.** The two components in the doublet at 350 keV could not be resolved in the presently analyzed spectra. AW used coincidence techniques to obtain the intensities of the two components. Differences between the level energies deduced in the present work give 350.095 and 350.207 keV for the  $\gamma$ -ray energies; using the relative intensities of AW gives an expected “center of gravity” of the combined peak at 350.182 keV, in excellent agreement with the presently measured value of  $350.186 \pm 0.010$  keV. Imposing an energy difference of 0.112 keV, based on the present deduced level energies, on the two components of the doublet gives the fitted energies and intensities listed in Table VIII.

**407.6 keV.** The presently deduced intensity for this  $\gamma$  ray is nearly double that reported by AW but agrees well with the value of SJ ( $0.37 \pm 0.04$ ). In the  $\gamma$ -ray spectrum reported by AW (Fig. 2 of their paper), the height of the 407.6-keV peak appears greater than would be expected if the intensity were equal to their reported value of 0.19 (for example, it appears roughly comparable to the height of the peak at 513.7 keV, which was assigned an intensity of 0.43 by AW).

**469- to 470-keV doublet.** AW obtained relative intensities for the two components of this doublet through coincidence measurements. Although the two components are not resolved in the present work, the fits to the doublet structure have proved quite robust and reproducible, and the results for the intensities disagree with those of AW but are in better agreement with

TABLE VIII. Energies and intensities of  $\gamma$  rays emitted in the decay of  $^{105}\text{Ru}$ .

Previous work <sup>a</sup>		Present work		Levels <sup>b</sup>	
<i>E</i> (keV)	<i>I</i>	<i>E</i> (keV)	<i>I</i>	Initial	Final
62.39 10	0.14 2	63.241 35	0.123 10	E	D
81.20 10	0.11 2	81.672 35	0.083 4	L	I
129.782 4	12.0 3	129.624 10	11.4 2	B	A
139.33 10	0.10 2	139.397 14	0.076 4	H	G
149.10 7	3.73 30	149.115 10	3.58 7	C	A
163.46 10	0.33 4	163.473 10	0.357 7	N	L
183.60 12	0.21 2	183.628 10	0.245 5	N	K
225.08 12	0.26 2	225.013 15	0.257 5	I	G
245.21 15	0.053 10	245.208 27	0.057 3	N	I
254.88 12	0.14 2	254.900 12	0.160 4	I	F
262.83 10	13.9 3	262.828 10	14.5 2	D	B
286.3 2	0.06 1	286.654 43	0.052 4	K	G
306.66 12	0.17 2	306.794 30	0.189 9	L	G
316.44 13	23.5 8	316.496 10	23.1 2	K	F
326.14 10	2.25 25	326.154 10	2.49 2	E	B
330.85 10	1.41 16	330.859 10	1.57 1	N	H
339.4 2	0.03 1	339.699 39	0.039 2	F	B
343.3 2	0.06 1	343.314 25	0.071 3	M	G
349.96 10	0.61 3	350.099 20	0.75 20	G	C
350.18 10	2.15 25	350.211 20	2.24 20	L	E
369.45 12	0.10 2	369.527 15	0.125 3	J	D
393.36 10	7.98 10	393.378 10	8.65 8	K	D
407.60 13	0.19 2	407.570 10	0.335 4	R	N
413.53 10	4.76 40	413.538 10	5.18 5	L	D
469.37 10	37.1 11	469.347 10	38.3 3	F	A
470.12 30	0.39 5	470.235 20	1.75 15	N	G
479.6 2	0.059 2	478.808 25	0.073 3		
489.48 10	1.16 13	489.500 10	1.25 1	H	C
499.26 30	4.34 50	499.210 10	4.91 5	G	A
500.1 2	1.17 16	500.114 32	0.410 34	N	F
513.73 10	0.43 10	513.623 10	0.484 5	N	E
539.29 10	0.24 2	539.094 12	0.411 5	Q	L
559.24 10	0.23 2	559.245 12	0.248 4	Q	K
572	0.02 1	572.078 49	0.045 3		
575.07 12	1.80 20	575.106 10	2.06 2	I	C
576.96 30	0.04 1	577.019 13	0.226 4	N	D
591.20 15	0.17 2	591.161 12	0.171 3	R	K
597.10 15	0.063 15	597.058 31	0.078 3	P	I
621.04 10	0.15 2	620.898 13	0.157 5	Q	I
632.34 10	0.32 3	632.322 10	0.362 3	J	B
635.5 2	0.03 1	635.393 88	0.013 1	S	L
638.66 10	0.47 5	638.589 10	0.516 5	H	A
652.70 10	0.65 7	652.761 10	0.805 8	R	I
656.21 10	4.35 50	656.198 10	4.44 4	K	B
676.36 8	33.1 10	676.355 10	33.1 3	L	B
701.0 2	0.04 1	700.982 38	0.044 2	T	K
707 1	0.02 1	706.11 14	0.006 3	Q	H
724.31 8	100.0	724.211 10	100.0 10	I	A
738.27 10	0.16 2	738.379 10	0.188 2	R	H
805.84 15	0.096 20	805.973 14	0.101 1	L	A
820.0 2	0.03 1	820.229 45	0.0259 16	N	C
821.98 12	0.45 9	822.042 10	0.445 4	P	G
845.91 12	1.33 14	845.878 10	1.43 2	Q	G
846.9 2	0.06 1			O	F
851.98 10	0.33 4	851.927 10	0.325 3	P	F

TABLE VIII. (Continued.)

Previous work <sup>a</sup>		Present work		Levels <sup>b</sup>	
<i>E</i> (keV)	<i>I</i>	<i>E</i> (keV)	<i>I</i>	Initial	Final
875.85 15	5.29 20	875.728 10	5.59 5	Q	F
878.2 2	1.0 1	877.801 15	0.887 9	R	G
907.64 10	1.12 12	907.642 10	1.15 1	R	F
952.78 10	0.032 3	952.568 22	0.041 1	Q	D
969.44 10	4.45 15	969.414 10	4.46 4	N	A
977.9 2	0.004 1	977.884 42	0.007 1		
984.6 2	0.022 4	984.390 26	0.023 1	R	D
987.0 2	0.015 3	987.400 42	0.016 1	T	G
1017.47 10	0.68 7	1017.470 10	0.702 7	T	F
1059.6 2	0.057 15	1059.632 21	0.053 1	U	H
1082.7 2	0.017 4	1082.522 55	0.0125 8	W	H
1085.4 2	0.010 3	1085.531 62	0.0118 9	Y	I
1094	0.007 2	1094.433 124	0.0057 4	T	D
1172.58 20	0.016 4	1172.371 58	0.0181 9	P	C
1209.0 2	0.013 4	1209.302 52	0.0110 7	V	G
1215.38 10	0.15 2	1215.463 12	0.146 2	Q	B
1222.0 2	0.039 5	1221.979 31	0.041 1	W	G
1229.5 2	0.012 3	1228.730 66	0.0101 6	U	F
1238.8 2	0.004 1	1238.160 310	0.003 1	V	F
1251.89 15	0.041 5	1251.907 19	0.047 1	W	F
1321.26 10	0.43 5	1321.282 10	0.424 4	P	A
1340	0.001			Y	F
1357.2 2	0.005 1	1357.550 100	0.0047 6	T	B
1377.06 11	0.12 2	1377.017 10	0.112 2	R	A
1441.2 2	0.013 4	1441.420 39	0.0111 6	S	A
1448.3 2	0.011 3	1448.311 42	0.0147 9		
1571	0.002 1		<0.001	W	C
1698.1 2	0.16 3	1698.167 11	0.162 2	U	A
1708.7 2	0.0010 5		<0.002	V	A
1721.36 15	0.07 2	1721.149 13	0.0633 6	W	A
1765.4 3	0.0004 3		<0.001	X	A
1809	0.0005 4		<0.001	Y	A
1829.6 3	0.0016 12		<0.001	Z	A

<sup>a</sup>From NDS compilation [9].<sup>b</sup>See Table IX for identification of levels.

those of SJ ( $35.7 \pm 2.0$  and  $2.7 \pm 0.4$  for the two members of the doublet), also obtained from coincidence measurements.

*499- to 500-keV doublet.* A similar situation arises for this doublet: The present fits to the unresolved peaks disagree with the coincidence results of AW and agree better with those of SJ ( $4.90 \pm 0.24$  and  $0.61 \pm 0.10$ ).

*575- to 577-keV doublet.* This doublet is well resolved in the present spectra, but the fitted intensities disagree with those deduced by AW from coincidence data. As was the case with the unresolved doublets discussed above, the present intensities agree better with those of SJ ( $2.18 \pm 0.10$  and  $0.27 \pm 0.10$ ), also deduced from coincidence data.

*Unobserved transitions.* AW report several very weak transitions, with intensities of the order of 0.001. Those transitions were not observed in the present work, but (except for 846.9 keV) the upper limits on their intensities are generally at or above the intensities previously reported. The present study is therefore able neither to confirm nor to reject those transitions and the corresponding levels.

TABLE IX. Energy levels of  $^{105}\text{Rh}$  populated in the decay of  $^{105}\text{Ru}$ .

Level	Previous work <sup>a</sup>				Present work		
	$E$ (keV)	$J^\pi$	$I_\beta$ (%)	$\text{Log } ft$	$E$ (keV)	$I_\beta$ (%)	$\text{Log } ft$
A	0.0	$7/2^+$	<0.02	>10.4	0.000	0.00	
B	129.781 4	$1/2^-$	2.6 10	8.13 22	129.624 10	0.5 5	8.8 5
C	149.19 5	$9/2^+$			149.115 10	<0.05	>9.8
D	392.65 5	$3/2^-$	0.5 3	8.6 4	392.452 14	0.16 11	9.1 3
E	455.61 6	$5/2^-$	<0.2	>8.9	455.768 13	<0.16	>9.0
F	469.38 5	$(3/2)^+$	2.1 7	7.86 15	469.346 10	3.05 20	7.70 3
G	499.31 5	$5/2^+$	0.5 3	8.4 4	499.210 10	0.20 4	8.84 9
H	638.68 5	$7/2^+$			638.600 10	<0.02	>9.7
I	724.33 5	$5/2^+$	47.8 6	6.175 8	724.221 10	48.3 5	6.171 7
J	762.11 8	$3/2^-$	0.199 18	8.50 4	761.956 12	0.232 5	8.44 1
K	785.93 5	$(1/2^+)$	16.9 6	6.540 17	785.833 10	17.1 2	6.535 7
L	805.94 5	$3/2^+$	18.8 6	6.464 15	805.975 10	19.2 2	6.455 7
M	842.61 21		0.028 5	9.24 8	842.524 27	0.034 2	9.15 3
N	969.45 5	$(5/2^+)$	3.98 15	6.881 18	969.435 10	4.41 10	6.837 12
O	1316.28 21		0.028 5	8.32 8	1316.28 21 <sup>a</sup>	0.029 5	8.31 8
P	1321.36 6	$(5/2^+)$	0.61 6	6.97 5	1321.275 10	0.615 6	6.970 9
Q	1345.27 5	$(3/2)^+$	3.52 13	6.149 19	1345.082 10	3.83 6	6.114 11
R	1377.06 5	$(3/2^+)$	1.63 9	6.40 3	1376.994 10	1.75 2	6.368 10
S	1441.33 15	$(3/2^+, 5/2)$	0.020 3	8.12 11	1441.412 36	0.0115 5	8.361 22
T	1486.81 9	$(3/2^+)$	0.35 4	6.73 6	1486.804 13	0.368 4	6.709 12
U	1698.43 12	$(3/2^+, 5/2)$	0.108 16	6.28 7	1698.177 10	0.107 1	6.286 20
V	1708.41 12	$(3/2^+, 5/2)$	0.0085 20	7.32 11	1708.483 52	0.0072 7	7.39 5
W	1721.32 9	$(5/2^+)$	0.080 11	6.26 7	1721.177 10	0.0786 8	6.267 22
X	1765.4 3	$(5/2^+, 3/2^+)$	0.00019 15	8.5 + 7, -4	1765.4 3 <sup>a</sup>	<0.0003	>8.3
Y	1809.74 21	$(5/2, 3/2^+)$	0.0054 15	6.61 13	1809.752 63	0.0063 7	6.54 6
Z	1829.6 3	$(5/2^+)$			1829.6 3 <sup>a</sup>	<0.0005	>7.4

<sup>a</sup>From NDS compilation [9].

Based on the presently measured  $\gamma$ -ray energies, an error minimization procedure has produced a best set of level energies, which are listed in Table IX and compared with the previously adopted set from the NDS [9]. The present work is unable to improve on the energies for the 1765.4- and 1829.6-keV levels because no radiations emitted from those levels were observed. Of the 77  $\gamma$  rays observed in the present work that have been previously placed among the  $^{105}\text{Rh}$  levels, 52 (=67%) fit between the assigned levels within 1 standard deviation and 65 (=84%) fit within 2 standard deviations, suggesting that the uncertainties have been neither overestimated nor underestimated by a significant factor.

One notable exception occurs for the 572.1-keV transition. AW also reported a weak transition at 572 keV. With the present improved energy measurement for this transition, it does not fit in its previously assigned location in the decay scheme (1376.998 keV to 805.983 keV, for which  $\Delta E = 571.019$  keV). The measured  $\gamma$ -ray energy disagrees with the level energy difference by some 20 standard deviations. The placement is therefore doubtful, but there is no other placement in the presently accepted level scheme that matches the observed energy.

AW proposed a level at 1448 keV deexcited by  $\gamma$  rays of energy 1448.3, 977.9, and 479.6 keV. These three  $\gamma$  rays were also observed in the present work but cannot all be fit into the assigned levels. If the 1448.311-keV transition

depopulates a level at 1448.311 keV, then we would expect the transition to the level at 469.346 keV to have an energy of 978.965 keV, which disagrees with the measured  $\gamma$ -ray energy of 977.884 keV by 18 standard deviations. The transition from the proposed 1448.311-keV level to 969.435 keV would have an energy of 478.876 keV, which is in reasonable agreement with the measured energy of 478.808 keV (but it should be noted that another possible placement of this transition would be from 1321.275 to 842.524 keV, with  $\Delta E = 478.751$  keV). The present work thus can neither strongly confirm nor disprove the existence of the proposed level at 1448 keV.

#### D. $^{105}\text{Rh}$ decay

$^{105}\text{Rh}$ , which is produced following the decay of  $^{105}\text{Ru}$ , is itself radioactive and decays with a half-life of 1.47 d to levels of  $^{105}\text{Pd}$ . Table X shows the presently measured  $\gamma$ -ray energies and intensities for this decay, in comparison with the previous values from the NDS [9], which are based on the measurements reported by Schriber and Johns [31]. The corresponding level energies of  $^{105}\text{Pd}$  are shown in Table XI. Because all of the four  $\gamma$  rays observed in the present work decay directly from an excited state to the ground state, the level energies are directly determined from the  $\gamma$ -ray energies. The previously measured

TABLE X. Energies and intensities of  $\gamma$  rays emitted in the decay of  $^{105}\text{Rh}$ .

Previous work <sup>a</sup>		Present work		Levels <sup>b</sup>	
$E$ (keV)	$I$	$E$ (keV)	$I$	Initial	Final
38.72 3	0.13 2			D	B
280.1 2	0.87 7	280.523 10	0.905 9	B	A
306.1 2	26.7 15	306.311 10	27.6 3	C	A
318.9 1	100	319.231 10	100.0 10	D	A
442.8 7	0.22 3	442.417 10	0.210 2	E	A

<sup>a</sup>From NDS compilation [9].<sup>b</sup>See Table IX for identification of levels.

38.72-keV transition connects levels with an energy difference, based on the presently proposed energy values, of 38.708 keV, which is in excellent agreement with the measured energy. Table XI shows  $\log ft$  values deduced from the presently measured  $\gamma$ -ray intensities, assuming the NDS value of 75.0% for the  $\beta$  intensity feeding the ground state.

### E. $^{96}\text{Tc}$ decay

Table XII shows the present results for some of the more intense  $\gamma$  rays emitted in the decay of 4.28-d  $^{96}\text{Tc}$ . A summary of the previously measured  $\gamma$ -ray energies and intensities may be found in the NDS [34], taken mostly from the measurements reported by Barrette *et al.* [35]. A more precise determination of the  $\gamma$ -ray energies in the  $^{96}\text{Mo}$  daughter was obtained from the decay of  $^{96}\text{Nb}$  by Meyer [36]. The present results are comparable to the more precise results of Meyer and a significant improvement over the previous  $^{96}\text{Tc}$  decay results.

## V. DISCUSSION AND CONCLUSIONS

The lack of agreement among the various measurements of the  $^{96}\text{Ru}$  thermal cross section is at first troubling. However, any comparison of the various experimental results must be done with a critical examination of the parameters used in the analysis and how their limits of uncertainty affect the uncertainty of the deduced cross section. The absolute intensities of the strongest  $\gamma$  rays in the  $^{97,103,105}\text{Ru}$  decay schemes are uncertain by about 1%, which is typical of many decay scheme studies (flux monitor decays of  $^{60}\text{Co}$  and  $^{198}\text{Au}$  are atypical in that they exceed this level of precision by a considerable factor). Debertin and Helmer [37] assert that the best achievable uncertainty in the efficiency calibration of Ge

TABLE XII. Energies and intensities of some  $\gamma$  rays in  $^{96}\text{Mo}$  emitted in the decays of  $^{96}\text{Tc}$  and  $^{96}\text{Nb}$ .

Previous work <sup>a</sup>		Previous work <sup>b</sup>		Present work	
$(^{96}\text{Tc} \text{ decay})$		$(^{96}\text{Nb} \text{ decay})$		$E$ (keV)	$I$
$E$ (keV)	$I$	$E$ (keV)			
778.22 4	100	778.224 15	778.224 10	100 1	
812.54 4	82.2 35	812.581 15	812.577 10	81.7 8	
849.86 4	97.8 38	849.929 13	849.893 10	98 1	
1091.30 4	1.10 8	1091.349 12	1091.325 12	1.09 2	
1126.85 6	15.2 12	1126.965 21	1126.910 10	15.2 2	
1200.17 8	0.37 3	1200.231 13	1200.226 14	0.39 1	
1441.14 10	0.054 6	1441.129 24	1441.042 75	0.065 3	
1497.72 10	0.093 7	1497.807 15	1497.661 69	0.086 5	

<sup>a</sup>From NDS compilation [34].<sup>b</sup>From Meyer [36].

detectors is about 0.5% under optimal conditions; taking a more conservative view, allowing for possibly less than optimal conditions, the uncertainty in efficiency determinations may be no better than 1%. Although recent measurements have considerably improved the uncertainty limits, at the time of the previous Ru cross-section measurements, the accepted  $^{97}\text{Ru}$  half-life was  $2.9 \pm 0.1$  d, an uncertainty of 3.4%. According to the Commission on Isotopic Abundances and Atomic Weights [38], between 1980 and the present time the recommended  $^{96}\text{Ru}$  isotopic abundance changed from  $0.0552 \pm 0.0005$  to  $0.0554 \pm 0.0014$ ; this increase in the uncertainty reflects an attempt to account for the variability of Ru content in terrestrial samples [12]. The corresponding changes over this same period in the abundances of the other stable Ru isotopes relevant to this work are  $0.316 \pm 0.002$  to  $0.3155 \pm 0.0014$  for  $^{102}\text{Ru}$  and  $0.187 \pm 0.002$  to  $0.1862 \pm 0.0027$  for  $^{104}\text{Ru}$ . Thus, even ignoring uncertainties introduced in the neutron flux determinations, the uncertainties discussed in the preceding would combine to give a net uncertainty in the  $^{96}\text{Ru}$  cross section of 3.8% using the 1980 values of the abundance and half-life and 2.9% using the current values. Depending on the relative contribution of epithermals to the neutron spectrum, the uncertainty in the resonance integral can also contribute to the uncertainty in the deduced thermal cross section (and  $^{96}\text{Ru}$  is especially sensitive to the uncertainty in the resonance integral because of the relatively large ratio of  $I$  to  $\sigma$ ). Adjusting the  $^{96}\text{Ru}$  cross section to account for the changes in the

TABLE XI. Energy levels of  $^{105}\text{Pd}$  populated in the decay of  $^{105}\text{Rh}$ .

Level	Previous work <sup>a</sup>				Present work		
	$E$ (keV)	$J^\pi$	$I_\beta$ (%)	$\log ft$	$E$ (keV)	$I_\beta$ (%)	$\log ft$
A	0.000	5/2 <sup>+</sup>	75.0 6	5.728 9	0.000	75.0 6 <sup>a</sup>	5.728 8
B	280.51 22	3/2 <sup>+</sup>			280.523 10	<0.05	>7.9
C	306.25 3	7/2 <sup>+</sup>	5.2 4	5.76 4	306.311 10	5.37 13	5.747 18
D	319.216 24	5/2 <sup>+</sup>	19.7 5	5.112 21	319.231 10	19.6 5	5.114 18
E	442.38 4	(7/2 <sup>+</sup> )	0.042 6	6.83 7	442.417 10	0.0401 9	6.86 3

<sup>a</sup>From NDS compilation [9].



accepted values of the half-life and abundance reduces Heft's value from 0.218 b to perhaps 0.212 b and the value of De Corte and Simonits from 0.229 b to about 0.223 b. (These corrections cannot be done exactly without more information about the details of the previous experiments.) If the uncertainties in these two previous values are increased according to the preceding discussion, then the present value and these two corrected values (along with the previous value of Katcoff and Williams, which has a much larger uncertainty) form a consistent set with an unweighted average of 0.214 b and an uncertainty of around 0.010 b.

Of the two larger previously reported values of the  $^{96}\text{Ru}$  thermal cross section, the measurement reported by Halperin and Druschel exceeds the consensus of the four smaller values by about 2 standard deviations, while the value of Rambaek and Steinnes exceeds it by almost 4 standard deviations. Halperin and Druschel used a Ru sample enriched to 67% in  $^{96}\text{Ru}$  and observed the resulting decays with a NaI detector. In their experiments the Cd ratio was about 2; that is, the activity produced by thermal + epithermal captures was roughly double that produced by epithermals alone, suggesting that the thermal and epithermal capture rates were about equal. As a result the deduced thermal cross section is extraordinarily sensitive to the value of the resonance integral. The resonance integral obtained by Halperin and Druschel is smaller than those deduced in all other reported studies; had they deduced a larger resonance integral, they would have obtained a correspondingly smaller thermal cross

section. The Ru experiments of Rambaek and Steinnes used Ru of natural isotopic abundance [39]. In their analyses, both of these experiments used a half-life that is larger than the current value (2.88 d by Halperin and Druschel and 2.9 d by Rambaek and Steinnes) and a 216-keV branching ratio that is larger than the present value (0.90 and 0.91). Replacing their half-life with the current value would tend to decrease their deduced thermal cross sections, while replacing their branching ratio with the current value would tend to increase them. However, it is not possible in retrospect to determine the exact amount of the increase or decrease nor which correction would have the greater effect on their result.

There is good overall agreement of the results of various measurements of the  $^{102}\text{Ru}$  thermal cross section. In the case of  $^{104}\text{Ru}$ , the present value agrees well with all previous values except that of Rambaek and Steinnes, which differs from the other experiments in that it was the only one to use the daughter  $^{105}\text{Rh}$   $\gamma$  rays (rather than the direct  $^{105}\text{Ru}$  decays) in the analysis.

#### ACKNOWLEDGMENTS

The support of the staff and facilities of the Oregon State University Radiation Center in carrying out these experiments is acknowledged with gratitude. I am grateful for the assistance of Jon Rambaek in communicating the details of his 1976 experiments.

- 
- [1] T. Bereznai, D. Bodizs, and G. Keömley, *J. Radioanal. Chem.* **36**, 509 (1977).
- [2] R. Gijbels and J. Zels, *J. Radioanal. Chem.* **35**, 115 (1977).
- [3] S. F. Mughabghab, *Atlas of Neutron Resonances: Resonance Parameters and Thermal Cross Sections Z = 1–100* (Elsevier, Amsterdam, 2006).
- [4] EXFOR/CSISRS Experimental Nuclear Reaction Data, National Nuclear Data Center, Brookhaven National Laboratory (<http://www.nndc.bnl.gov/exfor/exfor00.htm>).
- [5] <http://radiationcenter.oregonstate.edu/>.
- [6] ORTEC, Inc. – <http://www.ortec-online.com/pdf/a65.pdf>.
- [7] A. Artna-Cohen, *Nuclear Data Sheets* **70**, 85 (1993).
- [8] D. De Frenne and E. Jacobs, *Nucl. Data Sheets* **93**, 447 (2001); see also D. De Frenne, *ibid.* **110**, 2081 (2009).
- [9] D. De Frenne and E. Jacobs, *Nucl. Data Sheets* **105**, 775 (2005).
- [10] Evaluated Nuclear Structure Data File, National Nuclear Data Center, Brookhaven National Laboratory (<http://www.nndc.bnl.gov/ensdf/>).
- [11] J. R. Goodwin, V. V. Golovko, V. E. Iacob, and J. C. Hardy, *Phys. Rev. C* **80**, 045501 (2009).
- [12] J. R. de Laeter, J. K. Böhlke, P. De Bièvre, H. Hidaka, H. S. Peiser, K. J. R. Rosman, and P. D. P. Taylor, *Pure Appl. Chem.* **75**, 683 (2003).
- [13] C. H. Wescott, W. H. Walker, and T. K. Alexander, in *Proceedings of the Second United Nations International Conference on the Peaceful Uses of Atomic Energy* (United Nations, Geneva, 1958), Vol. 16, p. 70.
- [14] P. A. Aarnio, J. T. Routti, and J. V. Sandberg, *J. Radioanal. Nucl. Chem.* **124**, 457 (1988).
- [15] R. G. Helmer and C. van der Leun, *Nucl. Instrum. Methods Phys. Res. A* **450**, 35 (2000).
- [16] S. Katcoff and D. C. Williams, *J. Inorg. Nucl. Chem.* **7**, 194 (1958).
- [17] J. Halperin and R. E. Druschel, Oak Ridge National Laboratory Report No. ORNL-3832, 1965, p. 5.
- [18] J. F. Rambaek and E. Steinnes, International Atomic Energy Agency Report No. INDC(SEC)-62/L, 1977, p. 151.
- [19] R. E. Heft, in *Conference on Computers in Activation Analysis*, edited by R. Farmakes (American Nuclear Society, La Grange Park, IL, 1978).
- [20] F. De Corte and A. Simonits, *J. Radioanal. Nucl. Chem.* **133**, 43 (1989).
- [21] P. M. Lantz, Oak Ridge National Laboratory Report No. ORNL-3832, 1965, p. 6.
- [22] H. Ishikawa, *J. Nucl. Sci. Technol.* **6**, 587 (1969).
- [23] P. Lantz, Oak Ridge National Laboratory Report No. ORNL-3679, 1964, p. 11.
- [24] V. A. Anufriev, S. I. Babich, N. G. Kocherygin, and V. N. Nefedov, *At. Energ.* **58**, 279 (1985).
- [25] W. B. Cook, L. Schellenberg, and M. W. Johns, *Can. J. Phys.* **48**, 217 (1970).
- [26] M. E. Phelps and D. G. Sarantites, *Nucl. Phys. A* **171**, 44 (1971).
- [27] B. W. Huber and K. Krämer, *Z. Phys.* **267**, 111 (1974).
- [28] E. S. Macias, M. E. Phelps, D. G. Sarantites, and R. A. Meyer, *Phys. Rev. C* **14**, 639 (1976).
- [29] B. Chand, J. Goswamy, D. Mehta, S. Singh, M. L. Garg, N. Singh, and P. N. Trehan, *Nucl. Instrum. Methods Phys. Res. A* **273**, 310 (1988).

- [30] N. K. Aras and W. B. Walters, *Phys. Rev. C* **11**, 927 (1975).
- [31] S. O. Schriber and M. W. Johns, *Nucl. Phys. A* **96**, 337 (1967).
- [32] H. G. Börner, W. F. Davidson, J. Almeida, J. Blanchot, J. A. Pinston, and P. H. M. van Assche, *Nucl. Instrum. Methods* **164**, 579 (1979).
- [33] J. B. Wilhelmy, Ph.D. thesis, University of California, 1969.
- [34] L. K. Peker, *Nucl. Data Sheets* **68**, 165 (1993).
- [35] J. Barrette, M. Barrette, A. Boutard, R. Haroutunian, G. Lamoureux, G. Renaud, and S. Monaro, *Nucl. Phys. A* **172**, 41 (1971).
- [36] R. A. Meyer, *Fizika* **22**, 153 (1990).
- [37] K. Debertin and R. G. Helmer, *Gamma- and X-Ray Spectrometry with Semiconductor Detectors* (North-Holland, Amsterdam, 1988), p. 224.
- [38] <http://www.ciaaw.org/>.
- [39] J. Rambaek (private communication).